

# Total Variance Constrained Electrical Properties Tomography Using a 16-channel Transceiver Array Coil at 7T

Yicun Wang<sup>1</sup>, Xiaotong Zhang<sup>1</sup>, Jiaen Liu<sup>1</sup>, Pierre-Francois Van de Moortele<sup>2</sup>, and Bin He<sup>1,3</sup>

<sup>1</sup>Department of Biomedical Engineering, University of Minnesota, Minneapolis, Minnesota, United States, <sup>2</sup>Center for Magnetic Resonance Research, University of Minnesota, Minneapolis, Minnesota, United States, <sup>3</sup>Institute for Engineering in Medicine, University of Minnesota, Minneapolis, Minnesota, United States

**Introduction:** Electrical Properties Tomography (EPT) can be used to extract the conductivity and permittivity distribution of tissue *in vivo*. However, most existing studies are based on Helmholtz equation, making assumptions of local homogeneity, which resulted in severe reconstruction artifacts on tissue boundary.<sup>1-4</sup> Other gradient based algorithms either required manually assigned “integration seed point”<sup>5</sup> and “boundary conditions”,<sup>6</sup> or additional dielectrical padding to create a second RF distribution.<sup>6</sup> In this study, we introduced a novel approach to reconstruct electrical properties with a 16-channel transmit/receive coil at 7T by fitting measured  $B_1$  maps regularized by total variance. Simulation and physical phantom results show high accuracy and robustness of this new method.

**Theory:** A partial differential equation (1) is derived starting from the Maxwell’s Equations, where  $\tilde{B}_1^+$  is the RF transmit field at angular Larmor frequency  $\omega$ ;  $\mu_0$  is the magnetic permeability constant;  $\tilde{\epsilon} = \epsilon_r \epsilon_0 - i \frac{\sigma}{\omega}$  is the complex electrical properties, with  $\epsilon_r$  being relative permittivity and  $\sigma$  being electrical conductivity.  $\tilde{B}_z$  is minimized with a stripline design of the RF coil<sup>7</sup>, thus ignored in the equation. Equation (2) is derived by introducing a parameter transformation  $\tilde{\gamma} = \frac{1}{\tilde{\epsilon}}$  and omitting the variation of  $\tilde{\epsilon}$  along  $z$  direction.<sup>6</sup> By replacing the spatial derivatives of  $\tilde{\gamma}$  with its central difference approximation, a complex linear system of equations (3) is obtained with  $N$  being the pixel number in a 2D image. Equation (3) is solved by minimizing residue squares regularized by total variance of the complex EP map, as defined in (4) and (5).

**Methods:** *Simulation* 3D DUKE head model was loaded into a 16-channel transmit/receive array coil<sup>7</sup> at 7T and the RF field was simulated in finite-difference time-domain (FDTD) based software SEMCAD.  $\tilde{B}_1^+$  map of each coil element was retracted directly from the simulation. *Phantom Experiment* A single compartment cylinder phantom with a diameter of 8.7 cm and length of 20cm was constructed composed of distilled water, NaCl, gelatin and CuSO<sub>4</sub>·5H<sub>2</sub>O (mass ratio 100:0.12:3:0.025), and the EP measured as  $\sigma = 0.34$  S/m,  $\epsilon_r = 77$  with Agilent 85070D dielectric probe kit and an Agilent E4991A network analyzer at 298MHz. The phantom was placed in the head coil with its long axis aligned with the main magnetic field direction. The experiment was performed in a 7T magnet (MagnexScientific, UK) driven by a Siemens console (Erlangen, Germany). A 16-channel transmit/receive head coil was used for both RF transmit and signal receive.<sup>7</sup> Hybrid  $B_1$  mapping method<sup>8-10</sup> was employed to obtain the absolute magnitude of transmit and receive  $B_1$  for each coil element, as well as the relative phase map between them, with a spatial resolution of 1.5x1.5x3 mm<sup>3</sup>. Gauss’s Law for magnetism was then utilized to retrieve the absolute transmit and receive phase for each coil element.<sup>4</sup> *Image Reconstruction* The  $\tilde{B}_1^+$  maps from 16 channels were added directly or with a phase shim, e.g. by adding a constant phase step  $\pi/8$  to each channel, to produce two different  $\tilde{B}_1^+$  maps. Helmholtz equation was solved first to provide an initial guess of the EP distribution. Then nonlinear conjugate gradient method<sup>11</sup> was implemented to solve equation (5).

**Results:** Simulation results are shown in Figure 1 and Table 1. Both the reconstructed conductivity and the relative permittivity show high consistency with those in the target maps. We can observe residual inhomogeneity of reconstructed conductivity and permittivity in white matter in (d), which is due to weighting of equations in (3) imposed by inhomogeneous transmit  $B_1$  field. Phantom results are shown in Figure 2. Along y direction across the center of the phantom, the reconstructed conductivity is  $0.38 \pm 0.01$  S/m (mean  $\pm$  standard deviation) and the relative permittivity is  $76.8 \pm 0.70$ .

Table 1. Comparison of EP reconstruction with or without regularization

|                         | $\lambda = 0$ |                       | With optimized $\lambda$ |                       |
|-------------------------|---------------|-----------------------|--------------------------|-----------------------|
|                         | Conductivity  | Relative Permittivity | Conductivity             | Relative Permittivity |
| Relative Error          | 30.8%         | 22.4%                 | 15.6%                    | 13.4%                 |
| Correlation Coefficient | 0.848         | 0.536                 | 0.887                    | 0.839                 |

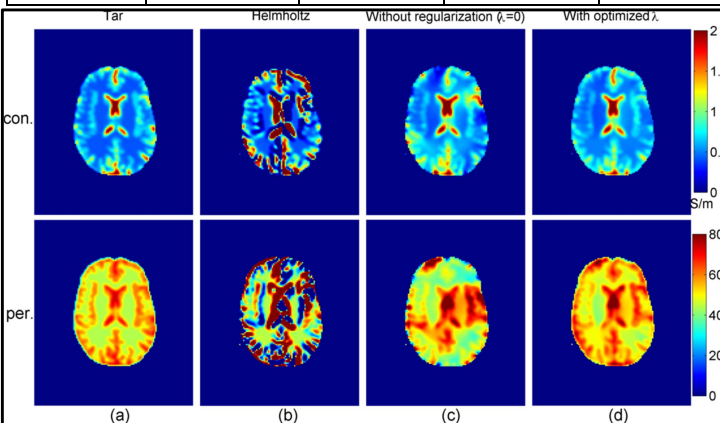


Figure 1. Simulation results, (a) target conductivity and relative permittivity, reconstructed (b) by Helmholtz equation (initial guess of the proposed algorithm), (c) without total variance regularization, (d) with optimized regularization coefficient.

$$\nabla^2 \tilde{B}_1^+ = -\omega^2 \mu_0 \tilde{B}_1^+ \tilde{\epsilon} + \left( \frac{\partial \tilde{B}_1^+}{\partial x} - i \frac{\partial \tilde{B}_1^+}{\partial y} \right) \left( \frac{\partial \tilde{\epsilon}}{\partial x} + i \frac{\partial \tilde{\epsilon}}{\partial y} \right) \frac{1}{\tilde{\epsilon}} + \frac{\partial \tilde{B}_1^+}{\partial z} \frac{\partial \tilde{\epsilon}}{\partial z} \frac{1}{\tilde{\epsilon}} \quad (1)$$

$$(\nabla^2 \tilde{B}_1^+) \tilde{\gamma} + \left( \frac{\partial \tilde{B}_1^+}{\partial x} - i \frac{\partial \tilde{B}_1^+}{\partial y} \right) \left( \frac{\partial \tilde{\gamma}}{\partial x} + i \frac{\partial \tilde{\gamma}}{\partial y} \right) = -\omega^2 \mu_0 \tilde{B}_1^+ \quad (2)$$

$$\tilde{E}_{(N,N)} \tilde{Y}_{(N,1)} = \tilde{C}_{(N,1)} \quad (3)$$

$$TV(\tilde{Y}_{(m,n)}) = \sum_{i=1}^{m-1} \sum_{j=1}^{n-1} \{ |\tilde{Y}_{i+1,j} - \tilde{Y}_{i,j}| + |\tilde{Y}_{i,j+1} - \tilde{Y}_{i,j}| \} \quad (4)$$

$$\text{minimize } \frac{1}{2} \left\| \tilde{E}_{(N,N)} \tilde{Y}_{(N,1)} - \tilde{C}_{(N,1)} \right\|_2^2 + \lambda TV(\tilde{Y}_{(m,n)}) \quad (5)$$

**Discussion and Conclusion:** In this study, a new algorithm was proposed by utilizing total variance which aims to extend the generality of EPT. Simulation and phantom experiment have demonstrated the feasibility of this new approach. This approach can also be adapted to EPT using quadrature coils that are clinically available.

**Acknowledgements:** NIH R21EB017069, R01EB006433, R21EB009133, R21EB014353, P30NS057091, U01HL117664, P41EB015894 and S10RR026783 of WM KECK Foundation.

**References:** [1] Katscher *et al.*, *IEEE TMI* 2009, 28:1365 [2] Wen, *Proc. SPIE* 2003, 5030:471 [3] Voigt T *et al.*, *ISMRM* 2011, 66: 456 [4] Zhang *et al.*, *MRM* 2013, 69: 1285 [5] Liu *et al.*, *MRM* (Online) [6] Hafalir *et al.*, *IEEE TMI* 2014, 33:777 [7] Adriany *et al.* *MRM* 2008, 59:590 [8] Van de Moortele *et al.*, *MRM* 2005, 54:1503 [9] Van de Moortele *et al.*, *ISMRM* 2007, 1676 [10] Van de Moortele *et al.*, *ISMRM* 2009, 367 [11] Lustig *et al.*, *MRM* 2007, 58: 1182

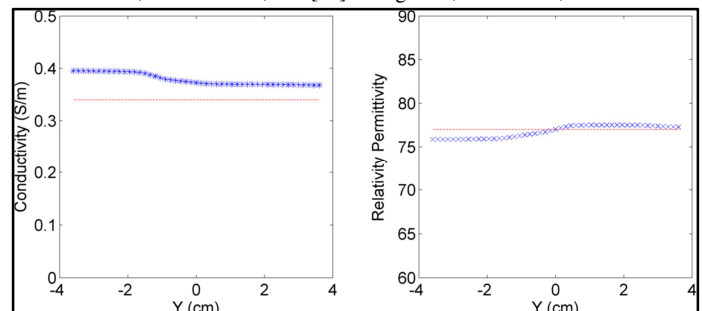


Figure 2. Reconstructed result along y direction on the central slice of the phantom.